Supplementary Information

VO_2(M)@SiO_2/Poly(N‑isopropylacrylamide) Hybrid Nanothermochromic Microgels for Smart Window

Yu Wang,[a] Fang zhao,[a] Jie Wang,[a] Ali Raza Khan,[a] Yulin Shi,[b] Zhang Chen,[c] Kaiqiang Zhang,[c] Li Li,[a] Yanfeng Gao,[cd*] Xuhong Guo[ab*]*

[a]State Key Laboratory of Chemical Engineering, East China University of Science and Technology, Shanghai 200237, China. E-mail: guoxuhong@ecust.edu.cn

[b]Engineering Research Center of Materials Chemical Engineering of Xinjiang Bingtuan, Key Laboratory of Materials Chemical Engineering of Xinjiang Uygur AutonomousRegion, Shihezi University, Shihezi 832000, China.

[c]School of Materials Science and Engineering, Shanghai University, Shanghai 200444, China.

[d]School of Materials Science and Energy Engineering, Foshan University, Foshan 528000, China.

[*]To whom correspondence should be addressed. E-mail: fzhao1@ecust.edu.cn (Fang Zhao, co-corresponding author), yfgao@shu.edu.cn (Yanfeng Gao, co-corresponding author), guoxuhong@ecust.edu.cn (Xuhong Guo, co-corresponding author)

1.1 The X-ray diffraction pattern of VO_2(M) and VO_2(M)@SiO_2

We verified the crystalline phase of VO_2 in nanoparticles (NPs) of VO_2(M) and VO_2(M)@SiO_2 by X-ray diffraction (XRD), respectively. As shown in Fig. S1, all the diffraction peaks of the VO_2(M)@SiO_2 sample corresponded to those of monoclinic VO_2(M) (JCPDS no.043-1051), without a broad reflection peak from 2θ=20° to 2θ=30° which can be assigned to non-uniformity of the SiO_2 shell. The unchanged XRD pattern also confirmed the chemical stability of VO_2(M) is stable during modifying process.

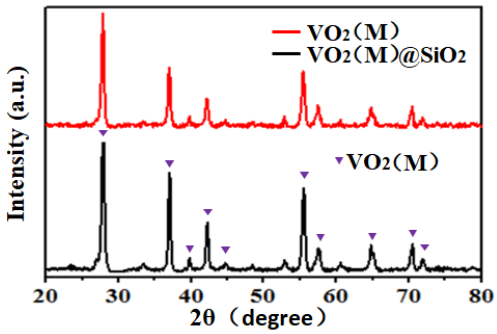

Figure S1. XRD results of the VO_2(M) NPs and VO_2(M)@SiO_2 NPs.

1.2 Effect of Surfactant Type on VO_2(M) Dispersion

Figs. S2 show the stability of solvent prepared with two kinds of surfactant: sodium dodecyl sulfate (SDS) and poly(vinylpyrolidone) (PVP). It can be seen that all the VO_2 NPs subsided in both SDS systems with two different contents of VO_2 NPs (Figs. S2a and b), while VO_2 NPs were all well dispersed in the existence of PVP polymer (Figs. S2c and d).

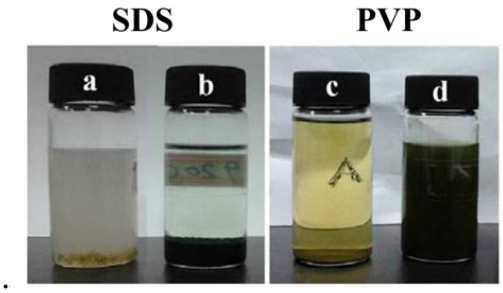

Figure S2. Composite microgels synthesized with different surfactants and varying amounts of VO_2(M) nanoparticles: (a) SDS, 0.05 wt% VO_2(M); (b) SDS, 0.1 wt% VO_2(M); (c) PVP, 0.05 wt% VO_2(M); (d) PVP, 0.1 wt% VO_2(M).

1.3 The transparent-opaque transition of the smart window

Before or after phase transition, all the hybrid microgels (samples I, II and III) were kept transparent and homogeneous, without any precipitation phenomenon. At room temperature, the hybrids were transparent, and brownish due to the existence of VO_2(M) NPs (left column of Fig. S3). The color of films changed with VO_2(M) content: the higher the VO_2(M) content was, the deeper the brownish color was.

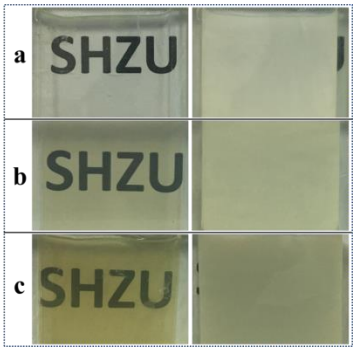

Figure S3. Pictures of different hybrid microgel samples (a) sample I, (b) sample II, (c) sample III at 20 ℃ (left column) and 50 ℃ (right column).

1.4 The phase transition behavior of VO_2 and VO_2@SiO_2

The pure VO_2(M) nanoparticles was synthesized through a “heating-up” process, According to the DSC (Differential scanning calorimeter) results, The phase transition began at 60 ℃ and ended at 100 ℃. The latent heat during the insulator-to-metal transition (IMT) of VO_2(M) NPs is around 43 J g^{-1}. This high crystal quality will achieve strong solar energy regulation ability. The transition temperature of the nanoparticle remained unchanged after being coated by SiO_2 (VO_2(M)@SiO_2, solid lines).

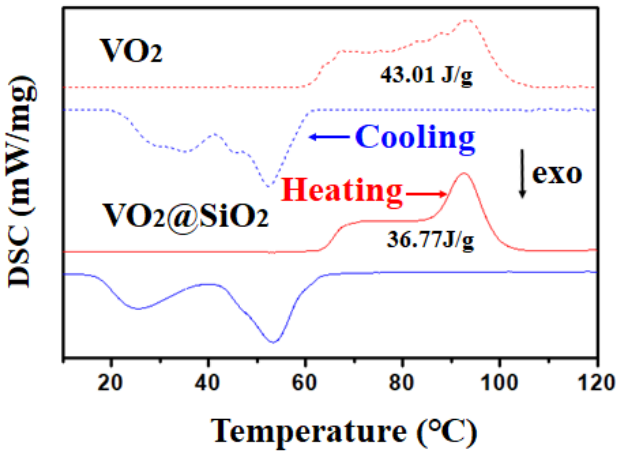

Figure S4. DSC curves as function of temperature upon heating (red lines) or cooling (blue lines) for VO_2 (dashed lines) and VO_2@SiO_2 (solid lines). The latent heat of VO_2 and VO_2@SiO_2 are shown as the inserts.

1.5 The optical performance of Sample I, II and III and pure PNIPAm microgel

Optical properties between pure PNIPAm microgel and hybrids (Sample I, II and III) are shown in Table S1.

Table S1. Comparison of the optical properties for Sample I, II, III with PNIPAm microgel.

Sample	$T_{lum,low}$ (%)	$T_{lum,high}$ (%)	$\triangle T_{lum}$ (%)	$T_{lum,average}$ (%)	$\triangle T_{IR}$ (%)	$\triangle T_{sol}$ (%)
PNIPAm	67.0	1.6	65.3	34.3	29.4	64.9
Sample I	72.7	1.7	71.0	37.2	26.7	64.9
Sample II	59.7	1.3	58.4	30.5	23.4	55.3
Sample III	75.6	1.3	74.3	38.4	22.4	62.7

1.6 TEM image of hybrids with 4 g/L PVP content

As shown in Fig. S5, there existed a thick gel layer which was caused by the high content of PVP. Therefore, a high PVP concentration will influence the hybrid structure and make the structure change from microgel to large-sized hydrogel to some extent. The large-size hydrogel shows a long response time and a relatively small reduction of transmission in both visible and IR ranges after phase transition, as reported by the literatures (Zhou, Y; Cai, Y.-F.; Hu, X.; Long, Y. Temperature-responsive hydrogel with ultra-large solar modulation and high luminous transmission for “smart window” applications. *J. Mater. Chem. A* **2014**, *2*, 13550-13555.). Thus a high PVP concentration is not favorable for achieving good optical performance of the hybrid microgel.

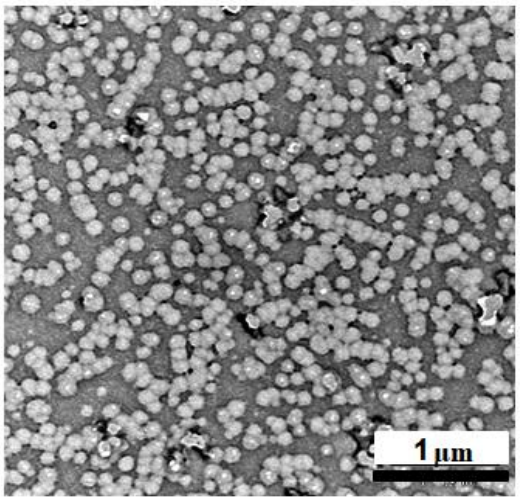

Figure S5. TEM image of hybrids obtained from 4 g/L PVP content.

1.7 Comparison of optical performance of previously reported results and my hybrid sample

As shown in Table, comparing with the result of given reviews, our composite film shows the excellent solar modulation properties (62.7%) with high luminous transmittance (75.6%). But we also have some short comings, the high solar modulation properties sacrificed the luminous transmittance at high temperature, which means that we need extra energy to keep visible transmittance for views.

Table S2. Comparison of our hybrid sample with other thermochromic materials ("-" means data is not available).

Category	Sub-category	Material content	Modulated solar spectrum (nm)	T_{lum}(%)	$\triangle T_{sol}$(%)	Ref.
Unhybridized system	VO_2	VO_2	700-2500	45.6	22.3	1
		W+Zr-doped VO_2	700-2500	56.4	12.3	2
	Hydrogel	PNIPAm	250-2200	70.7	25.5	3
		Modified cellulose	250-2200	67.4	25.7	4
		Modified starch	250-2200	87.7	40.1	5
	Metamaterial	Kiri-Kirigami metamaterials	200-2200	-	-	6
	Perovskite	Halide perovskite	400-700	-	-	7
	Liquid crystal	-	400-2200	-	-	8
VO_2-based hybrid system	The other material is non-thermal-responsive	VO_2/PU	700-2500	45.6	22.3	1
		VO_2/Si-Al gel	700-2500	59.1	12	9
		VO_2/PDMS	700-2500	85	-	10
		VO_2/TiO_2	700-2500	61.2	14.6	11
	The other material is thermal-responsive	VO_2/PNIPAm	250-2500	62.6	34.7	12
		VO_2/HPC	250-2500	56	36	13
		VO_2/NLETS	500-2500	71	18.2	14
		Our composite VO_2@SiO_2/PNIPAm	250-2500	75.6	62.7	This work

1.8 References

(1) Chen, Z.; Gao, Y.; Kang, L.; Cao, C.; Chen, S.; Luo, H. Fine crystalline VO_2 nanoparticles: Synthesis, abnormal phase transition temperatures and excellent optical properties of a derived VO_2 nanocomposite foil. *J. Mater. Chem. A.* **2014**, 2, 2718-2727.

(2) Shen, N.; Chen, S.; Chen, Z.; Liu, X.; Cao, C.; Dong, B.; Luo, H.; Liu, J.; Gao, Y. The synthesis and performance of Zr-doped and W–Zr-codoped VO_2 nanoparticles and derived flexible foils. *J. Mater. Chem. A.* **2014**, 2, 15087-15093.

(3) Zhou, Y.; Cai, Y.; Hu, X.; Long, Y. Temperature-responsive hydrogel with ultra-

large solar modulation and high luminous transmission for “smart window” applications. *J. Mater. Chem. A.* **2014**, 2, 13550-13555.

(4) Yang, Y.-S.; Zhou, Y.; Yin Chiang, F. B.; Long, Y. Temperature-responsive hydroxypropylcellulose based thermochromic material and its smart window application. *RSC Adv.* **2016**, 6, 61449-61453.

(5) Zhang, K.; Shi, Y.; Wu, L.; Chen, L.; Wei, T.; Jia, X.; Chen, Z.; Li, M.; Xu, Y.; Wang, Y.; Gao, Y.; Guo, X. Thermo- and pH-responsive starch derivatives for smart window. *Carbohydr. Polym.* **2018**, 196, 209-216.

(6) Tang, Y.; Lin, G.; Yang, S.; Yi, Y. K.; Kamien, R. D.; Yin, J. Programmable Kiri-Kirigami Metamaterials. *Adv. Mater.* **2017**, 29, 1604262.

(7) Lin, J.; Lai, M.; Dou, L.; Kley, C. S.; Chen, H.; Peng, F.; Sun, J.; Lu, D.; Hawks, S. A.; Xie, C.; Cui, F.; Alivisatos, A. P.; Limmer, D. T.; Yang, P. Thermochromic halide perovskite solar cells. *Nat. Mater.* **2018**, 17, 261-267.

(8) Liang, X.; Guo, S.; Chen, M.; Li, C.; Wang, Q.; Zou, C.; Zhang, C.; Zhang, L.; Guo, S.; Yang, H. A temperature and electric field-responsive flexible smart film with full broadband optical modulation. *Mater. Horiz.* **2017**, 4, 878-884.

(9) Liu, C.; Cao, X.; Kamyshny, A.; Law, J. Y.; Magdassi, S.; Long, Y. VO(2)/Si-Al gel nanocomposite thermochromic smart foils: largely enhanced luminous transmittance and solar modulation. *J. Colloid Interface Sci.* **2014**, 427, 49-53.

(10) Moot, T.; Palin, C.; Mitran, S.; Cahoon, J. F.; Lopez, R. Designing Plasmon-Enhanced Thermochromic Films Using a Vanadium Dioxide Nanoparticle Elastomeric Composite. *Adv. Opt. Mater.* **2016**, 4, 578-583.

(11) Chen, Z.; Cao, C.; Chen, S.; Luo, H.; Gao, Y. Crystallised mesoporous TiO_2(A)–VO_2(M/R) nanocomposite films with self-cleaning and excellent thermochromic properties. *J. Mater. Chem. A.* **2014**, 2, 11874-11884.

(12) Zhou, Y.; Cai, Y.; Hu, X.; Long, Y., VO_2/hydrogel hybrid nanothermochromic material with ultra-high solar modulation and luminous transmission. *J. Mater. Chem. A.* **2015**, 3, 1121-1126.

(13) Yang, Y.-S.; Zhou, Y.; Chiang, F. B. Y.; Long, Y. Tungsten doped VO_2/microgels hybrid thermochromic material and its smart window application. *RSC Adv.* **2017**, 7, 7758-7762.

(14) Zhu, J.; Huang, A.; Ma, H.; Chen, Y.; Zhang, S.; Ji, S.; Bao, S.; Jin, P. Hybrid films of VO_2 nanoparticles and a nickel(ii)-based ligand exchange thermochromic system: excellent optical performance with a temperature responsive colour change. *New J. Chem.* **2017**, 41, 830-835.